Mechanical Properties of Hydroxyapatite-Filled Ethylene Vinyl Acetate Copolymer Composites: Effect of Particle Size and Morphology

Shiny Velayudhan,[1] P. Ramesh,[1] H. K. Varma[2]

[1]*Polymer Processing Laboratory Biomedical Technology wing, Sree Chitra Tirunal Institute for Medical Sciences and Technology, Trivandrum 695 012, Kerala, India*
[2]*Bioceramic Laboratory Biomedical Technology wing, Sree Chitra Tirunal Institute for Medical Sciences and Technology, Trivandrum 695 012, Kerala, India*

Received 2 February 2010; accepted 17 May 2010
DOI 10.1002/app.32812
Published online 19 August 2010 in Wiley Online Library (wileyonlinelibrary.com).

ABSTRACT: Pliable and bioactive composites made of hydroxyapatite (HAP) and ethylene vinyl acetate (EVA) copolymer were developed for the repair of defective cranium. This article describes the mechanical properties of HAP–EVA composites. The effects of HAP particle size and morphology of HAP on the properties of resultant composites were investigated using various techniques. It was found that the composites containing smaller HAP particles had higher values of tensile modulus, flexural modulus, and impact strength. Examination of the fracture surfaces revealed that only a mechanical bond existed between the filler and the matrix. © 2010 Wiley Periodicals, Inc. J Appl Polym Sci 119: 1594–1601, 2011

Key words: ceramics; polymer–matrix composites; mechanical properties; impact properties; cranioplasty

INTRODUCTION

In the last few decades, polymer–hydroxyapatite (HAP) composites have attracted much interest as they exhibit some measure of structural and mechanical equivalence to natural bone. Literature reports many polymer–HAP systems intended for various applications.[1–6] Ethylene vinyl acetate (EVA) copolymer–HAP composites represent one such system that has shown great potential for repairing/augmenting deformities of cranium.[7–9] Implantation studies of these composites in rabbits have shown them to be completely biocompatible [7] and osteoconductive.[10]

The two most important requirements that an ideal cranioplastic implant should meet are (i) bioactivity, i.e., the ability of the material to integrate with the bone tissue in contact with it by forming ultrastructural chemical bonds and (ii) malleability, i.e., the ease in shaping the implants intraoperatively to fit the complex topography of the skull defect. It has been identified that a bioactive material facilitates early fixation of the prosthesis onto the bone and improves the prosthesis lifetime even if the biomechanical mismatch of the implant and the tissue remains.[11] EVA–HAP composite thus makes a next to ideal material for cranioplasty as they encompass both the properties of bioactivity and malleability. Presence of HAP, a calcium phosphate ceramic similar in composition to the mineral phase of bone, imparts bioactivity and promotes bone apposition to the surface rather than encouraging bone resorption.[12] EVA copolymer on the other hand is a biocompatible polymer[13,14] that has been used in various biomedical applications such as drug delivery, coatings of the Kirschner wire used as intramedullary nails for fixing fractures in the bone, [15] and coatings of intravascular stents [16] and pressure-sensitive adhesive tape for the damaged skin.[17] The thermoplastic-elastomeric and amorphous nature of EVA allows incorporation of high quantities of filler without substantial loss of its ductility. The combination of bioactive ceramic HAP and thermoplastic elastomer EVA has two distinctive advantages: (1) the presence of HAP improves the mechanical properties of the composite and also makes the composite bioactive, and (2) the presence of EVA would render the composite malleable and facilitate precise sculpting of the composite according to the defect formed/created in the skull. Development of HAP–EVA composite can thus be expected to give a promising material for cranioplasty. This article reports the preparation and mechanical property evaluation of the novel HAP–EVA composites. The composite behavior with respect to HAP particle size and loading under tensile, bending, and impact mechanical loading is discussed.

Correspondence to: P. Ramesh (rameshsct@yahoo.com or rameshp@sctimst.ac.in).

TABLE I
Properties of Ethylene Vinyl Acetate (EVA) Copolymers

Polymer grade	E18	E28
Vinyl acetate content (wt %)[a]	18	28
Melt flow index {g/(10 min^{-1})}[a]	2	25
Density (g/cc)[a]	0.93	0.95

[a] Data were taken from manufacturer's product data sheet.

MATERIALS AND METHODS

Materials

Ethylene vinyl acetate copolymers

Two grades of EVA copolymers, E18 and E28 (Shriswasan Chemicals (M), Mumbai, India), were used as received; their properties are detailed in Table I.

Hydroxyapatite

Two grades of synthetic HAP namely spray-dried HAP (H_s) and freeze-dried HAP (H_f) were also used. Both the grades of HAP were synthesized in the laboratory by a precipitation route involving ammoniated calcium nitrate and ammonium hydrogen phosphate solutions, following the established procedure.[8,18] The HAP synthesized was characterized for the particle size (Malvern Mastersizer 2000 particle size analyzer, Malvern Instrument, UK) and surface morphology (JOEL JSM-5400 scanning electron microscope). The mean particle size ($d_{0.5}$), particle size distribution, and specific surface area of the HAP grades used for the study are given in Table II. The synthesized HAP powders were found to have a broad monomodal particle size distribution, with mean particle size of 5.8 μm (for H_s) and 49.2 μm (for H_f). Both powders had significant amounts of submicroscopic-sized particles. The differences in the morphology of the HAP grades can be seen in the scanning electron micrographs of the two powders in Figure 1(a,b). The spray-dried powder [Fig. 1(a)] had spherical morphology, whereas the freeze-dried powder exhibited irregular morphology and was found as agglomerates of submicron HAP crystallites [Fig. 1(b)].

Preparation of the composites

The cryogenically ground EVA powder was blended with predried HAP powder (dried at 100°C for 2 h) in a domestic blender for about 15 min. The HAP–EVA composites containing 10, 20, 30, and 40 vol % of HAP were prepared using E28 polymer matrix. Composites with 40 vol % of HAP were prepared from E18 polymer matrix. The designations and compositions of the composites prepared for the study are given in Table III. The blended powder was then melted and mixed in a torque rheometer (Polylab Rheomix 600, Haake, Germany) attached with a 120 cc mixing chamber. The temperature of the mixing chamber was maintained at 140 and 120°C, respectively, for composites fabricated from E18 and E28. Counter-rotating cam rotor with rotor speed of 40 rpm was used throughout the compounding process. The mixing time was 6 min, and at the end of which the HAP–EVA composites were dumped out of the torque rheometer and compression molded in a laboratory model hydraulic press (Santhosh Industries, Mumbai). The temperature and pressure used for the compression molding varied from 120–150°C and 20–100 kg/(sq cm), respectively, depending upon the volume percentage of HAP loaded in the composite material.

The density of E18 and E28 was 0.93 and 0.95 g/cc, respectively. Theoretical density of 3.16 g/cc was assumed for HAP. These densities were used to calculate the weight required to produce the series of composites.

Filler distribution studies

The dispersion and distribution of HAP particles in the EVA matrix were investigated for E28H_s40 and E28H_f40 composites. The compression-molded E28H_s40 was microtomed and observed under transmission light microscope (Leitz, Germany). The composite E28H_f40 was fractured after immersing in liquid nitrogen, sputter coated with gold, and SEM examination was performed.

Determination of HAP content

The ash content of the various compression-molded composites was measured to quantify the amount of HAP in the composites. The specimen in the form of flakes was cut from random parts of molded composite plates, placed in dried and preweighed alumina crucibles, and burnt to ashes at 700°C in a muffle furnace for 24 h. After ashing, the specimens were cooled and stored in a desiccator. All weight measurements were carried out at room temperature in an electronic balance (LA 230S, Sartorius, Germany) having accuracy of ±0.1 mg. Ash contents were calculated as the percentage of the original specimen weight.

TABLE II
Particle Size and Particle Size Distribution of Hydroxyapatite Powders

Material code	Specific surface area (m^2 g^{-1})	Particle size (μm)		
		$d_{0.1}$	$d_{0.5}$	$d_{0.9}$
H_s	1.392	2.2	5.8	14.0
H_f	0.418	7.2	49.2	121.1

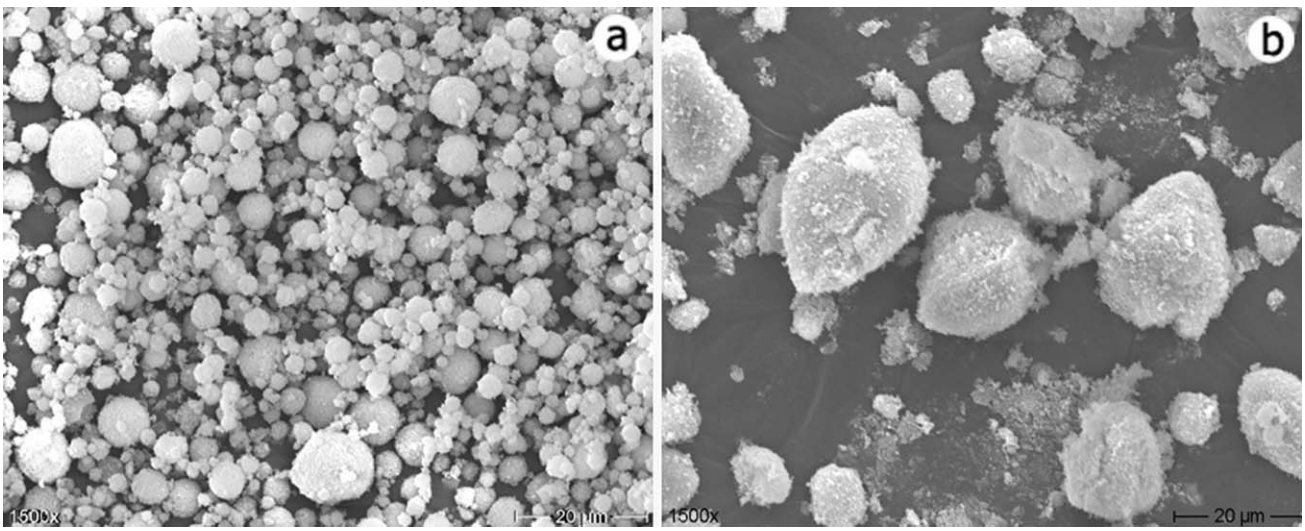

Figure 1 Scanning electron micrograph of (a) spray-dried and (b) freeze-dried hydroxyapatite powder.

Tensile properties

The specimens for tensile testing were punched out with a dumbbell die from compression-molded composite sheets. The specimen dimensions were in accordance with ISO 527 (Type A2). The tensile mechanical properties were measured using universal testing machine (Zwick 1485, Germany) at 22°C ± 2°C. The test was conducted according to the ISO 527-1:1993. The strain rate used for testing was 1 min^{-1}. Mean values were derived from tests performed on six dumbbell specimens.

Flexural properties

The flexural property analysis of the composite was carried out on a universal testing machine (Zwick 1485, Germany). The three-point bending method was used for this purpose. The distance between supports (span length) was 32 mm maintaining ASTM D 790-97 requirement. Rectangular specimens of dimensions (44 mm x 12.7 mm) were punched out from compression-molded composite plaques of 2-mm thickness. The specimens were lightly polished using 1000-grade silicon paper, followed by 4000-grade paper to improve the surface finish. A crosshead speed of 1 mm/min was used for the testing. Mean values were derived from tests performed on six rectangular bars.

Impact properties

Charpy impact test on unnotched specimens was conducted on Impact Tester (Ceast 6545, Italy) using a 158 J pendulum as per ISO 179-1:2000. Rectangular specimens of dimensions (80 mm x 10 mm) were punched out from 4-mm-thick compression-molded plaques, and the impact was executed in the edge-wise direction. The span length used was 60 ± 0.5 mm. At least six polished specimens were used for testing each composition of the composite material.

Fractography

The tensile fracture surfaces of the composite samples were examined in a scanning electron microscope at various magnifications.

RESULTS AND DISCUSSION

Composites processing

Composites with good dispersion and distribution of the particulate would eventually produce a consistent composite with isotropic properties. The photomicrographs [Fig. 2(a,b)] of the HAP–EVA composites indicate that the HAP particles are well

TABLE III
Designation and Composition of HAP–EVA Composites Used for the Study

Material code	Polymer matrix (vol %)		HAP (vol %)	
	E18	E28	H_f	H_s
E18	100	–	–	–
E28	–	100	–	–
E18H_f40	60	–	40	–
E18H_s40	60	–	–	40
E28H_f10	–	90	10	–
E28H_f20	–	80	20	–
E28H_f30	–	70	30	–
E28H_f40	–	60	40	–
E28H_s10	–	90	–	10
E28H_s20	–	80	–	20
E28H_s30	–	70	–	30
E28H_s40	–	60	–	40

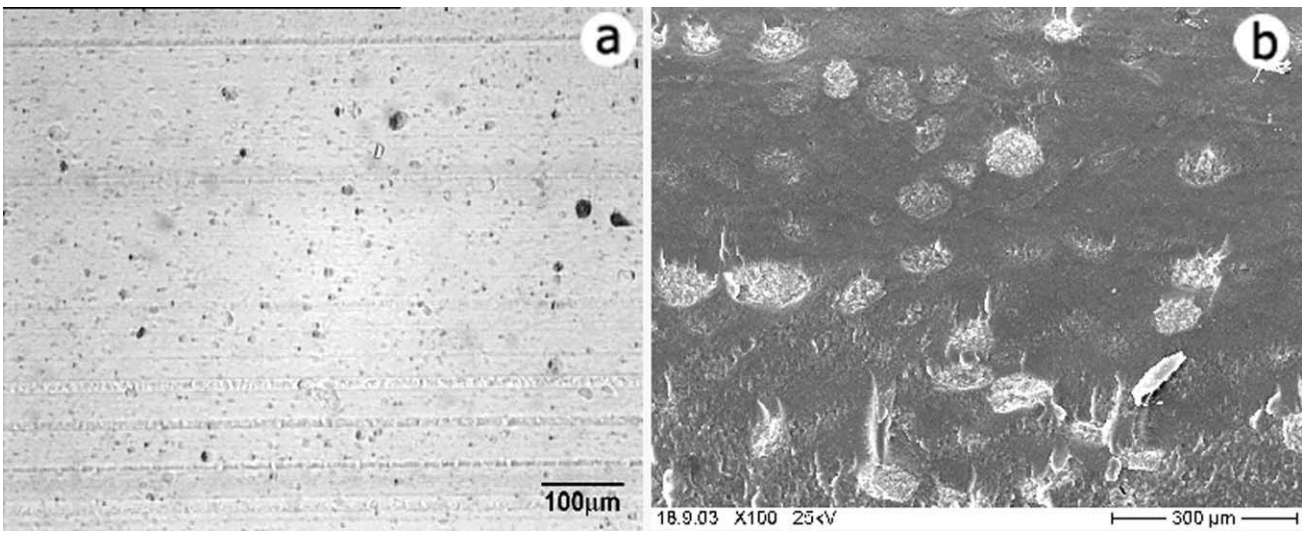

Figure 2 Distribution of HAP particles in E28 matrix at 40 vol % of HAP loading. (a) E28H_s40 and (b) E28H_f40.

distributed and dispersed in the polymer matrix. Furthermore, ashing analysis obtained (Table IV) of the molded specimens revealed loss of HAP particles less than 3 wt % using this processing route.

Tensile properties

Effect of HAP loading and particle size

It is clear from the tensile stress–strain curves of HAP–EVA composites, fabricated from E28, containing different volume fractions of HAP (Fig. 3). The HAP–EVA composite materials exhibited both ductile and brittle behavior, depending upon the amount of HAP incorporated into the EVA polymer. Unfilled EVA exhibits typical stress–strain curve of a soft and tough polymer material, characterized by low modulus and low yield stress, but very high elongation at break. The stress–stain curves for the composites with 10, 20, and 30 vol % HAP were also similar to that seen for E28. The strain at failure was, however, found to be decreasing with the increase in HAP loading. Necking was also noted for the composites with <30 vol % of HAP during tensile testing. For composite with 40 vol % HAP, the stress–strain curve showed linear elastic behavior followed by a plastic behavior without a sharp yield point, typical to highly filled elastomeric materials with rigid filler. It is worth mentioning that even at such high loading of HAP the material failed beyond the linear elastic region, indicating that the ductility of the composite was maintained. As the filler content increased, the recorded stress–strain curves became steeper and the elongation at break lower. The nature of the stress–strain curves at various loadings of HAP obtained for E28H_f40 was also similar to the ones recorded for E28H_s40, but at lower values of stress, strain, and modulus.

TABLE IV
Ashing Analysis Data Showing the Extent of HAP Incorporated in the HAP/EVA Composites

		HAP incorporated			
HAP (vol %)	HAP (wt %)	E28H_s	E28H_f	E18H_s	E18H_f
10	26.9	24.7	25.1	–	–
20	45.4	42.8	43.3	–	–
30	58.7	56.0	56.5	–	–
40	68.9	66.2	66.9	66.0	66.5

Effect of nature of polymer matrix

Figure 4 gives the stress–strain curves of E18, E18H_s40, and E18H_f40. The stress–strain curve of E18 is similar to that of E28, except that the fracture occurs at a higher stress and lower strain to fracture. The addition of 40 vol % of HAP affects the ductility of the composite catastrophically.

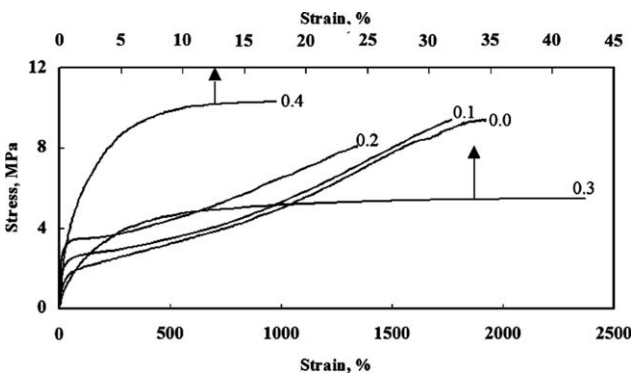

Figure 3 Tensile stress–strain curves for the composites fabricated from E28 at various volume fractions of spray-dried hydroxyapatite.

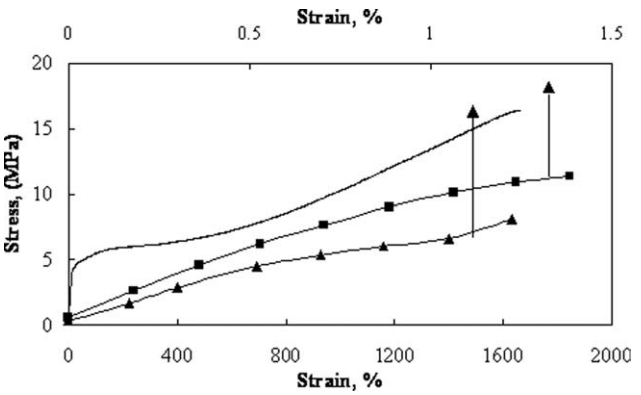

Figure 4 Stress–strain curves of HAP–EVA composites. (—) E18, (■) E18H_s40, and (▲) E18H_f40.

The values of tensile strength, Young's modulus, and strain to fracture of E28H_s40, E28H_f40, E18H_s40, E18H_f40, and the unfilled polymers (E28 and E18) are given in Table V. For the composites fabricated from both E28 and E18, addition of HAP led to increase in the values of Young's modulus with corresponding decrease in fracture strain. The values of tensile strength, however, showed a different trend. Although an increment in the tensile strength value was found in the case of E28, the value decreased for the composites fabricated from E18. The values of tensile strength and Young's modulus of E18H_s40 were, however, found to be higher than that of E28H_s40. The strain to fracture of E18H_s40, on the other hand, was lower than that of E28H_s40. Similar variation in tensile strength, Young's modulus, and strain to fracture was noted for E18H_f40 and E28H_f40.

Tensile fracture of filled polymer system such as HAP–EVA usually proceeds by a stage of cavitation where the matrix and the filler debond. The composite thus acts as a foam in this stage, and the ultimate strength of the system depends on the strength of this foam and the extent of any strain hardening capability that may occur in drawn polymer chains. The polymer matrices used in this study differed from each other in terms of vinyl acetate content and melt flow index. The E28 polymer matrix has a higher content of vinyl acetate and a higher value of MFI when compared with the E18 matrix polymer. A higher MFI value is associated with a lower value of molecular weight of the polymer. It has been reported that a high-molecular-weight polymer could be expected to have a greater strain hardening capability than the lower molecular grade and would consequently be capable of sustaining a higher load after cavitations have occurred.[19] This explains the higher values of tensile strength and Young's modulus of the composites fabricated from E18 when compared with those fabricated from E28.

TABLE V
Tensile Properties of HAP/EVA Composites

Material code	Tensile strength (MPa)	Young's modulus (MPa)	Strain at break (%)
E28	9.40 ± 0.19	12.00 ± 3.86	1923 ± 40
E28H_s40	10.34 ± 0.07	581.92 ± 3.82	17.58 ± 0.37
E28H_f40	7.26 ± 0.09	477.21 ± 2.56	10.66 ± 0.07
E18	16.34 ± 3.07	80.36 ± 2.43	1668 ± 68
E18H_s40	11.35 ± 0.12	820.50 ± 4.42	1.38 ± 0.02
E18H_f40	8.07 ± 0.05	732.20 ± 4.13	1.22 ± 0.03

TABLE VI
Flexural Properties of HAP–EVA Composites

Material code	Flexural strength (MPa)	Flexural modulus (GPa)	Flexural strain at break (%)
E28	3.01 ± 0.991	0.014 ± 0.01	11.12 ± 0.53
E28H_s40	17.62 ± 0.77	1.79 ± 0.09	4.52 ± 0.22
E28H_f40	14.62 ± 0.8	1.2 ± 0.04	4.76 ± 0.28
E18	3.12 ± 1.07	0.042 ± 0.03	6.15 ± 1.07
E18H_s40	20.65 ± 2.49	1.94 ± 0.08	2.45 ± 0.58
E18H_f40	19.92 ± 1.6	1.39 ± 0.12	4.6 ± 0.53

Flexural properties

Effect of HAP loading and particle size

The flexural strength, flexural modulus, and fracture strain of E28H_s40, E28H_f40, E18H_s40, E18H_f40, and the unfilled polymers (E28 and E18) are given in Table VI. The flexural modulus also showed considerable increase with corresponding decrease of strain at break. As expected, and similar to that found in tensile testing, the values of the flexural strength and flexural modulus were higher for composites containing smaller particle size HAP with both E18 and E28. However, the values of flexural strength and flexural modulus of the composites were higher than the corresponding values of tensile strength and tensile modulus. The tensile properties of materials are largely determined by the flaws and the submicroscopic cracks.[20] The cracks do not play such an important role in compression because the stresses tend to close the cracks rather than to open them. It is predicted that the compressive strengths of a material are nearly two to four times its tensile strength. In flexural tests, a part of the specimen is under tension and a part under compression. The compressive strengths being greater than the tensile strength, flexural strength tends to be greater than the tensile strengths.

Effect of nature of polymer matrix

The effect of nature of polymer matrix on the flexural strength, flexural modulus, and fracture strain of E28H_s40, E28H_f40, E18H_s40, E18H_f40, and the

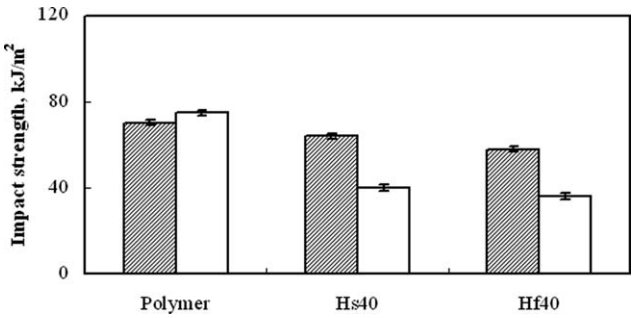

Figure 5 Impact strength of HAP–EVA composites fabricated from ■ E28 and □ E18 polymer matrices.

unfilled polymers (E28 and E18) is also evident from Table VI. Similar to that seen for the tensile properties, the composites fabricated from E18 recorded higher values for the flexural strength and flexural modulus, with a corresponding decrease in the values of strain to fracture.

Impact strength

Effect of filler particle size and nature

Figure 5 shows the unnotched Charpy impact test results of HAP–EVA composites fabricated from the two grades of HAP powders and two grades of polymers. It can be seen that both, the nature of HAP and the polymer matrix, affected the impact strength of the composites. Comparing the results for the two HAP powders, it shows that the composites fabricated from H_s have higher impact strength than those made from H_f, demonstrating better impact resistance of E28H_s40. Addition of HAP resulted in a decrease in the value of impact strength from 70.3 to 64 and 54.8 kJ/(sq m) for E28H_s40 and E28H_f40, respectively. Similar trend was noted for the composites fabricated from E18. The impact strength was decreased from 75 to 40.2 and 36 kJ/(sq m), respectively, for E18H_s40 and E18H_f40.

The different results caused by HAP types are due to their difference in particle size and surface morphology. Generally, the addition of mineral fillers will have an embrittling effect on polymers and decrease the impact energy.[21] However, mineral fillers can also act as toughners provided they meet certain requirements in terms of their particle size and morphology.[22-26] It has been reported that rigid spherical particles with smooth surface and particle size <5 μm, if dispersed homogeneously in the matrix polymer could improve the impact properties of composites.[23] In the case of rigid particles with irregular morphology and rough surfaces, the matrix cannot fill the rough surfaces as easily as the smooth ones, especially at some deep indents.[27] Therefore, more weak points exist in the composites with rough surfaced filler, resulting in poorer adhesion and a weaker interface between the filler and the matrix, which leads to easier debonding during impact test. This would explain the observed trend of increased impact strength of E28H_s40 compared with E28H_f40.

Effect of nature of polymer matrix

The effect of polymer matrix on the impact strength of the composites also showed some differences. In general, the higher the molecular weight of the polymer, the higher is the impact strength. This is evident from the values of impact strength of E18 and E28. However, contrary to that expected, the impact strength values obtained for E18H_s40 and E18H_f40 were far lower than E28H_s40 and E28H_f40. This is also clear from the tensile stress–strain curves recorded for these composites, which shows that both E18H_s40 and E18H_f40 undergo typical brittle mode of fracture. It has been reported that a large drop in the impact strength of higher molecular weight polymers occur when the filler particles restrict the flow and orientation of the polymer chains.[20] The restriction in orientation of the polymer chains disrupts the strain hardening capabilities of high-molecular-weight polymers resulting in

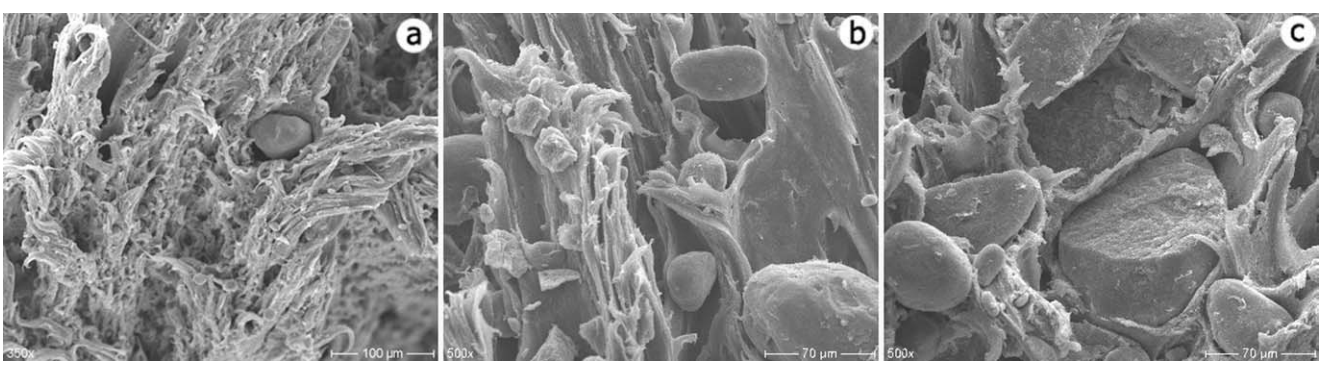

Figure 6 Tensile fracture morphology of HAP–EVA composites: (a) E28H_f20 (×350), (b) E28H_f40 (×350), and (c) E28H_f40 (×600).

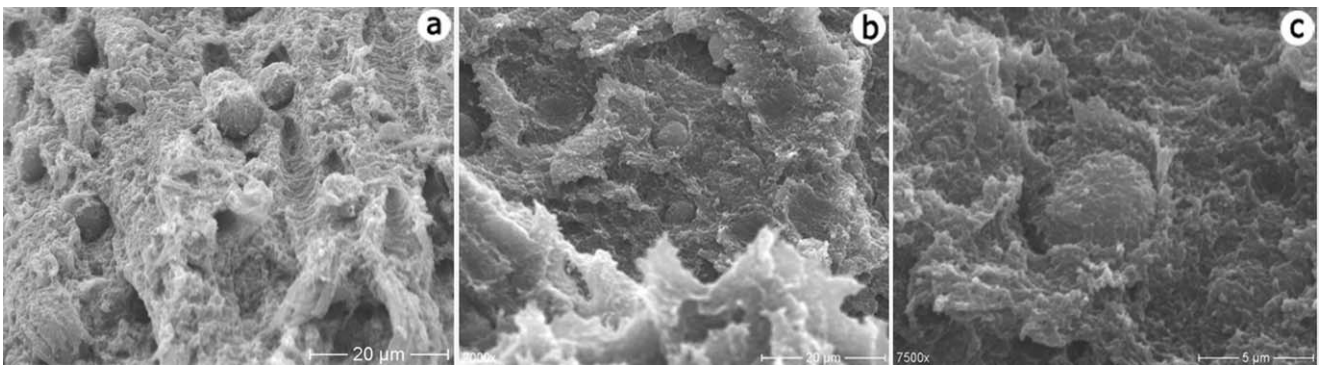

Figure 7 Tensile fracture morphology of HAP–EVA composites: (a) E28H_s40 (×1500), (b) E28H_s40 (×1000), and (c) E28H_s40 (×7500).

lower impact properties. This could be the possible reason for the lower impact values of E18H_s40 and E18H_f40 when compared with E28H_s40 and E28H_f40.

Fractography

The mechanical properties of the composites are influenced by the nature of the reinforcement used. This is evident from the tensile fractographs of the composites. Figure 6(a–c) shows the SEM images of tensile fracture surfaces of the HAP–EVA composites fabricated from the freeze-dried HAP particles at various volume percentage of HAP loading. The weak interaction of freeze-dried HAP–polymer is clear from this micrograph. The "relatively clean" surface of the particulate HAP reinforces this further. The fracture occurred mainly by the debonding of HAP particles from the matrix. The polymer matrix, however, underwent considerable deformation before fracture. Interestingly, in some areas, failure occurred by fracturing through the HAP particulate. The composites were fabricated using unsintered HAP particles. This makes the particles inherently weak and possibility of particle failure becomes higher, as the particle size is increased.

A different kind of fracture surface was noted in the case of composites fabricated from spray-dried HAP particles. The composites mainly fractured by debonding. However, unlike the composites fabricated from freeze-dried HAP particles, the spray-dried particulate HAP was found entangled and embedded in the polymer matrix [Fig. 7(a–c)]. Closer examination of the composites revealed the presence of traces of EVA polymer adhering to the surface of HAP particles at many areas, which explains the improved properties of the composites fabricated from the spray-dried HAP particulates.

CONCLUSIONS

The mechanical properties of HAP–EVA composites were evaluated. The mechanical testing carried out namely tensile, flexural, and impact provided useful insights on the composite properties. Generally, the composites fabricated from smaller particle size HAP (H_s) showed improved properties compared with the higher particle size (H_f) counterpart. The fractographs of the composites showed that the polymer matrix underwent considerable deformation before the fracture. The composites fabricated from smaller particle size HAP (H_s) seemed to be interacting better with the polymer matrix when compared with the freeze-dried particles.

A part of this work was carried out at Institute of Composite Materials (IVW), Kaiserslautern, Germany. The authors are grateful to Prof. K. Friedrich for the support and encouragement. The financial support from Department of Science and Technology (India) is also acknowledged.

References

1. Doyle, C.; Luklinska, Z. B.; Tanner, K. E.; Bonfield, W. Clin Imp Mat 1990, 9, 339.
2. Mangano, C.; Scarano, A.; Martinelli, R.; Piattelli, M.; Piattelli, A. J Dent Res 1997, 76, 1137.
3. Andronescu, E.; Momete, D. C.; Vasilescu, D. S. Silicates Ind 1999, 64, 187.
4. Woo, K. M.; Zhang, R. Y.; Deng, H. Y.; Ma, P. X. Abst Pap Am Chem Soc 2001, 222, U422.
5. Hunt, J. A.; Callaghan, J. T. Knee Surg Sports Traumatol Arthrosc 2008, 16, 655.
6. Xiao, X.; Liu, R.; Huang, Q. J Mater Sci Mater Med 2008, 19, 3429.
7. Velayudhan, S.; Anilkumar, T. V.; Kumary, T. V.; Mohanan, P. V.; Fernandez, A. C.; Varma, H. K.; Ramesh, P. Acta Biomater 2005, 1, 201.
8. Velayudhan, S.; Ramesh, P.; Varma, H. K.; Friedrich, K. Mater Chem Phys 2005, 89, 454.
9. Velayudhan, S.; Ramesh, P.; Varma, H. K.; Schmitt, S.; Friedrich, K. Compos Part A: Appl Sci Manuf 2007, 38, 1621.
10. Velayudhan, S., Ramesh, P., Varma, H. K. To appear.
11. Bonfield, W.European White Book on Fundamental Research in Materials Science, 1st ed.; Ruehl, M., Ed.; MPG Press: Munich, 2003; pp 72–76.
12. Jarcho, M. Clin Orthop Relat Res 1981, 157, 259.
13. Siegel, R. A.; Langer, R. Pharm Res 1984, 1, 2.

14. Shvarts, S.; Besinque, K.; Atkinson, R.; Gill, M. A. J Cont Ed 2002, 11.
15. Wong, W. C.; Yu, Y.; Wallace, A. L.; Gianoutsos, M. P.; Sonnabend, D. H.; Walsh, W. R. ANZ J Surg 2003, 73, 1022.
16. Pinchuk, L.; Nott, S.; Schwarz, M.; Kamath, K.U.S. Pat. 6,545,097(2000).
17. Ohmori, S.; Sugiyama, Y.; Morimoto, Y. Biol Pharm Bull 2001, 24, 78.
18. Varma, H. K.; Sivakumar, R. Phosphorus Res Bull 1996, 6, 35.
19. Hogg, P. J.; Behiri, J.; Brandwood, A.; Bowman, J.; Bonfiled, W. Proc Comp Biomed Eng 1985, 29, 1.
20. Nielsen, L. E. Mechanical Properties of Polymers and Composites; Marcel Dekker: New York, 1974; Vol. 2.
21. Bartczakm, Z.; Argon, A. S.; Cohen, R. E.; Weinberg, M. Polymer 1999, 40, 2347.
22. Zuiderduin, W. C. J.; Westzaan, C.; Huetink, J.; Gaymans, R. J. Polymer 2003, 44, 261.
23. Kim, G. M.; Michler, G. H. Polymer 1998, 39, 5689.
24. Wang, Y.; Lu, J.; Wang, G. J. J Appl Polym Sci 1997, 64, 1275.
25. Hoffmann, H.; Grellmann, W.; Zilvar, V. Polymer Composites; Walter de Gruyter: New York, 1986.
26. Liu, Z. H.; Kwok, K. W.; Li, R. K. Y.; Choy, C. L. Polymer 2002, 43, 2501.
27. Zhang, Y.; Tanner, K. E. Proceedings of the 18th European Conference on Biomaterials, Stuttgart, Germany, 122.